



Published in final edited form as:

Nat Immunol. 2009 September ; 10(9): 1026–1033. doi:10.1038/ni.1773.

***Deaf1* isoforms control the expression of genes encoding peripheral tissue antigens in the pancreatic lymph nodes during type 1 diabetes**

Linda Yip¹, Leon Su¹, Deqiao Sheng¹, Pearl Chang¹, Mark Atkinson², Margaret Czesak³, Paul R. Albert³, Ai-Ris Collier⁴, Shannon J. Turley⁴, C. Garrison Fathman¹, and Rémi J. Creusot¹

¹ Department of Medicine, Division of Immunology and Rheumatology, Stanford University School of Medicine, Stanford, California, 94305, USA

² Department of Pathology, University of Florida, Gainesville, FL, 32610, USA

³ Ottawa Health Research Institute (Neuroscience) and Department of Cellular and Molecular Medicine, University of Ottawa, Ottawa, Ontario K1H 8M5, Canada

⁴ Department of Cancer Immunology and AIDS, Dana Farber Cancer Institute, Boston, Massachusetts, 02115, USA

Abstract

Type 1 diabetes (T1D) may result from a breakdown in peripheral tolerance that is partially controlled by peripheral tissue antigen (PTA) expression in lymph nodes. Here we show that the transcriptional regulator deformed epidermal autoregulatory factor 1 (*Deaf1*) controls PTA gene expression in the pancreatic lymph nodes (PLN). The expression of canonical *Deaf1* was reduced, while that of an alternatively spliced variant was increased during the onset of destructive insulinitis in the PLN of NOD mice. An equivalent variant *Deaf1* isoform was identified in the PLN of T1D patients. Both NOD and human *Deaf1* variant isoforms suppressed PTA expression by inhibiting the transcriptional activity of canonical *Deaf1*. Reduced PTA expression resulting from the alternative splicing of *Deaf1* may contribute to T1D pathogenesis.

Users may view, print, copy, and download text and data-mine the content in such documents, for the purposes of academic research, subject always to the full Conditions of use:http://www.nature.com/authors/editorial_policies/license.html#terms

Correspondence should be addressed to C.G.F. (cfathman@stanford.edu).

Database Accession Numbers:

Microarray data comparing gene expression in the PLN of BALB/c *Deaf1*-KO mice to BALB/c mice are found at the NCBI GEO Database (series GSE13163). The mRNA sequence of DF1, DF1-VAR and Hu-DF1-VAR are available at NCBI Genbank: *DF1*- Accession FJ377319; *DF1-VAR1*- Accession FJ377318; Hu-DF1-VAR1- Accession FJ985253.

Author Contributions

L.Y. performed the microarray and QPCR assays, cloned the full length DF1-VAR1 and Hu-DF1-VAR isoform, synthesized the DF1-VAR1, Hu-DF1, and Hu-DF1-VAR fusion proteins, performed subcellular localization and siRNA experiments, assessed *Deaf1*-KO mice for lymphocyte infiltration and serum auto-antibodies, prepared the manuscript and composed the figures. R.J.C. extracted tissues for microarray and QPCR assays, isolated cellular subsets from PLNs, and with P.C., isolated and immortalized the CD45⁺ cells. D.S. cloned the DF1 isoform and synthesized DF1 fusion proteins. M.A. (and nPOD) provided human PLN and spleen samples. M.C. and P.R.A. provided the *Deaf1*-KO mice, and provided guidance on *Deaf1*-KO mouse work. A.R.C. and S.J.T. provided expertise and guidance on the isolation of the CD45⁺ LNSE. L.S. performed the immunoblotting, co-immunoprecipitation and luciferase reporter assays, and with C.G.F, R.J.C. and L.Y., was involved in all aspects of the planning and direction of this work. All authors reviewed and edited the manuscript. C.G.F. provided the majority of the funding.

INTRODUCTION

Type 1 diabetes (T1D) results from the autoimmune destruction of pancreatic β -cells by self-reactive T cells in genetically susceptible individuals due to a breakdown in central and/or peripheral tolerance. Central tolerance is enforced by medullary thymic epithelial cells (mTECs) that ectopically express a range of peripheral tissue antigens (PTAs) under the transcriptional control of the autoimmune regulator, *Aire 1*. Most maturing thymocytes that express T cell receptors (TCRs) specific for these PTAs are deleted, but some self-reactive T cells escape to the periphery where additional tolerance mechanisms are in place to protect tissues from autoimmune attack. In addition to regulatory T cells, peripheral tolerance can be mediated by lymph node stromal cells (LNSCs) and extrathymic Aire-expressing cells (eTACs), which present PTA peptides on MHC molecules and engage autoreactive PTA-specific T cells, ultimately leading to their clonal deletion^{2–4}. The mechanism(s) that controls PTA expression in secondary lymphoid tissues are not completely understood.

We previously compared the gene expression in tissues from non-obese diabetic (NOD) mice, a model of T1D, to that of NOD.B10 mice, a congenic strain that does not develop disease⁵. We found that the expression of the gene encoding the transcriptional regulator deformed epidermal autoregulatory factor 1 (*Deaf1*) changed in parallel with the expression of genes encoding a number of islet-specific tissue antigens including insulin 1 (*Ins1*), insulin 2 (*Ins2*), glucagon (*Gcg*), pancreatitis-associated protein (*Pap*), pancreatic polypeptide (*Ppy*), and regenerating islet-derived alpha and gamma (*Reg3a* and *Reg3g*) in the pancreatic lymph nodes (PLN). The expression of *Deaf1* and genes encoding these islet-specific antigens was significantly downregulated in the PLN of NOD mice at the age of 12 weeks⁵, a time coincident with the onset of destructive insulinitis.

In addition, we demonstrated that *Deaf1* regulates the expression of certain PTA genes in lymph node stromal elements (LNSE). We found that *Deaf1* can be processed into at least two isoforms in the PLN of NOD mice: a canonical *Deaf1* isoform that can translocate to the nucleus and is required for PTA expression, and a splice variant that is expressed in the cytoplasm and inhibits the transcriptional activity of canonical *Deaf1*. Remarkably, expression of a similar alternatively spliced *Deaf1* isoform was significantly increased in the PLN of T1D patients.

Results

***Deaf1* isoforms and PTA expression in the NOD PLN**

Microarray analysis demonstrated that the expression of various pancreatic genes and *Deaf1* change in parallel over time in the PLN of NOD mice (Fig. 1a,b)⁵. Two probes (probe 1 and 2) that bind to *Deaf1* were present on the microarray, but only probe 1 revealed an expression profile similar to that of the pancreatic PTA genes (Fig. 1a). Probe 1 hybridizes to a *Deaf1* region spanning exon 6 and 7, while probe 2 hybridizes to a region within exon 11 (Fig. 1c). The discordant expression profiles revealed by the two probes suggested that more than one *Deaf1* isoform might exist in the PLN, and that the relative expression of the two isoforms might change with age.

PCR cloning and sequence analysis of *Deaf1* mRNA in PLN tissue identified the canonical mRNA (*DF1*; Genbank Accession FJ377319) as well as an alternatively spliced transcript containing an insertion between exons 6 and 7 (*DF1-VAR1*; Genbank Accession FJ377318; Fig. 1c) that results in disruption of the binding site of probe 1. Thus, changes in the expression of these two *Deaf1* isoforms could explain the discordant patterns of expression revealed by the two probes (Fig. 1b).

The microarray data (Fig. 1a) used a pool of PLN mRNA from 1.5 and 20 week old NOD.B10 mice as controls⁵. Next, we quantified *DF1* and *DF1-VAR1* expression in NOD and NOD.B10 mice at various ages by quantitative PCR (QPCR) (Fig. 2 and Supplementary Fig. 1 and 2). The Taqman probe for *DF1* spans exons 6 and 7, at the intronic insertion site, and the *DF1-VAR1* primer and probes were designed to hybridize within the intronic insertion (Supplementary Fig. 1).

DF1 and *DF1-VAR1* expression did not differ between the PLN of NOD and NOD.B10 mice at 4 weeks of age (Fig. 2a, b). However, at 12 weeks, *DF1* mRNA expression was downregulated and *DF1-VAR1* expression was upregulated specifically in the NOD PLN. In contrast, *Gapdh* mRNA expression did not differ between 12-week NOD vs. NOD.B10 PLN (Fig. 2c). The changes in *DF1* and *DF1-VAR1* gene expression appear specific to the PLN, as no significant change was observed in spleen tissues of 12-week old NOD and NOD.B10 (Fig. 2d).

Characterization of Deaf1 isoforms

Canonical *DF1* contains an N-terminal alanine-rich region, the SAND and ZF-MYND domains, a helix-loop-helix (HLH) domain, and nuclear localization (NLS) and nuclear export sequences (NES). The *DF1-VAR1* transcript contains part of intron 7, which introduces a premature stop codon that results in a truncated protein lacking part of the NLS as well as the HLH, NES and ZF-MYND domains. *DF1-VAR1* also contains a 42 bp deletion in the alanine-rich region (Fig. 1c).

DF1 is ~70 kDa and localized in the nucleus of HEK 293 cells (Fig. 3a, b). DF1-VAR1 is ~50 kDa and was distributed throughout the cytoplasm (Fig. 3a, b). Interestingly, transient co-expression of DF1 with DF1-VAR1 resulted in nuclear localization of some DF1-VAR1, as revealed by immunofluorescence (Fig. 3b). This finding was confirmed by immunoblot experiments (Fig. 3c). Co-immunoprecipitation studies using Flag-tagged DF1 and V5 epitope tagged DF1-VAR1 demonstrate that DF1 and DF1-VAR1 can interact (Fig. 3d). These data suggest that the DF1 and DF1-VAR1 form hetero-dimeric complexes that can shuttle DF1-VAR1 into the nucleus using the NLS domain of DF1.

The transcriptional activity of DF1 and DF1-VAR1 was examined using a 26 bp *Deaf1*-response element-luciferase reporter plasmid⁶. When transiently transfected into HEK 293 cells, DF1-EGFP induced greater luciferase reporter activity than DF1-VAR1-EGFP (Fig. 3e). The lower transcriptional activity of DF1-VAR1 may be due to its cytoplasmic localization and reduced ability to translocate to the nucleus (Fig. 3b). Co-transfection of DF1-VAR1 and DF1 resulted in substantially lower transcriptional activity than that of equivalent amounts of DF1 alone (Fig. 3f).

Analysis of *Deaf1*-deficient BALB/c mice

To examine the genes that are regulated by *Deaf1* in the PLN, whole genome microarrays were performed on *Deaf1*-deficient BALB/c PLN tissues. Approximately 300 genes were upregulated and 300 were downregulated by ~2.5 fold in *Deaf1*-KO mice compared to BALB/c controls (Fig. 4a; Supplementary Table 1 and 2). Interestingly, among the top 30 genes whose expression was downregulated in *Deaf1*-KO PLN, almost three-quarters were considered potential PTAs with expression limited to ≤ 5 tissues; in contrast less than a quarter of the middle 30 genes, whose expression was not changed in the *Deaf1*-KO mice, were expressed in ≤ 5 tissues (Supplementary Table 3). The genes regulated by *Deaf1* in the PLN did not appear to significantly overlap with genes regulated by *Aire* in eTACs (Supplementary Fig. 3).

Two *Aire*-regulated genes, *Ambp* and *Fgb*, were found among the top 20 downregulated genes in the PLN of *Deaf1*-KO mice. *Reg3g* and *Ppy*, which encode pancreas-specific antigens, are also regulated by *Aire* in the thymus¹. To accurately measure the expression *Reg3g*, *Ppy*, *Ambp* and *Fgb* in the PLN of *Deaf1*-KO and control mice, SYBR green QPCR assays were used. The specificity and amplification efficiencies of each assay were confirmed by RT-PCR, melting curve analysis and standard curves (Supplementary Fig. 4). The expression of *Reg3g*, *Ppy*, *Ambp* and *Fgb* was significantly lower in the PLN of *Deaf1*-KO mice than WT controls (Fig. 4b). Interestingly, the expression of these same genes was upregulated in the thymus of *Deaf1*-KO mice, possibly due to increased *Aire* mRNA expression in the thymus of *Deaf1*-KO mice (Fig. 4c); *Aire* mRNA quantities were not different in the PLN of *Deaf1*-KO and control mice (Fig. 4b). Surprisingly, *Ins2* mRNA in the PLN of *Deaf1*-KO and BALB/c control mice was found to be 30 to 1700-fold lower than that of NOD and NOD.B10 mice (Supplementary Fig. 5), and thus was not detected in our microarray analysis.

To determine if 30-week old *Deaf1*-KO mice exhibited signs of autoimmunity, we looked for lymphocyte infiltration in various tissues and for the presence of autoantibodies. Lymphocyte infiltration was not detected in the pancreas, salivary glands, thyroid, gut or kidney (data not shown). The serum of *Deaf1*-KO mice reacted with certain proteins (~15–25 kDa) in whole eye lysate (Fig. 4d), but not with lysates of any other tissues examined (brain, salivary gland, heart, lung, liver, kidney, pancreas, spleen, and gut). The autoantibodies in the *Deaf1*-KO serum reacted with the outer segment layer of the retina, similar to autoantibodies in *Aire*-KO mice¹ (Fig. 4e).

Influence of *Deaf1* isoforms on PTA expression

Next we silenced the expression of *Deaf1* in NIH 3T3 cells, which express endogenous *Deaf1*, *Ambp* and *Fgb*, using siRNA to examine *Deaf1*-mediated regulation of these PTAs. *Deaf1* siRNA significantly inhibited the expression of DF1-Flag as well as endogenous *Deaf1* in NIH 3T3 cells, demonstrating the specificity of the *Deaf1* siRNA (Fig. 5a,b). *Deaf1* siRNA, compared to nonsense siRNA, also resulted in a significant suppression of *Ambp* and *Fgb* expression (Fig. 5c). However, over-expression of *DF1* in NIH 3T3 cells did not upregulate the expression of *Fgb*, and only slightly increased the expression of *Ambp* (Supplementary Fig. 6). These data indicate that, while a decrease in DF1 expression can

reduce PTA gene expression, an increase in DF1 expression alone may not be sufficient to enhance PTA gene expression. This conclusion is supported by data in the NOD PLN where decreased *DF1* and increased *DF1-VAR1* expression in 12-week old NOD mice strongly correlated with significantly reduced PTA gene expression (Fig. 2 and 6a), whereas increased *DF1* expression detected in 20 week NOD PLN did not correlate with increased PTA gene expression (Fig. 6a).

Next we sought to identify the cell type(s) in which changes in *DF1-VAR1* expression occur in the 12-week NOD PLN. We found that *DF1-VAR1* expression was approximately 7-fold and 10-fold higher in LNSEs from 12 week old NOD PLN than in T cells and B cells from the same mice (Fig. 6b). Silencing of *Deaf1* in immortalized lymph node CD45⁺ cells from pooled lymph nodes of BALB/c mice resulted in a decrease in *Ambp* and *Fgb* mRNA expression (Fig. 6c,d). Similarly, overexpression of *DF1-VAR1* in these cells reduced *Ambp* and *Fgb* expression (Fig. 6e). Although overexpression of *DF1-VAR1* did not alter the expression of *DF1* (Fig. 6e), we propose that it interfered with the transcriptional activity of DF1 by interacting with and retaining it in the cytoplasm. Supporting this hypothesis, immunoblot experiments performed with nuclear and cytoplasmic extracts of HEK 293 cells transfected with *DF1-Flag* and/or *DF1-VAR1-EGFP* showed that the amount of cytoplasmic DF1 was higher and the amount of nuclear DF1 was lower in cells transfected with both DF1-VAR1 and DF1 compared to cells transfected with DF1 alone (Fig. 6f). These data suggest that DF1-VAR1 can reduce PTA gene expression by interacting with and retaining DF1 in the cytoplasm.

Alternatively spliced human *Deaf1* variant

To examine if an alternatively spliced variant of *DEAF1* is expressed in human PLN, RT-PCR was performed with human PLN cDNA as a template and primers that span the start and stop codons of the human *DEAF1* gene (Supplementary Table 4). These primers amplified the canonical human *DEAF1* transcript (*Hu-DF1*; Genbank Accession No. BC053322), as well as an alternatively spliced variant (*Hu-DF1-VAR*; Genbank Accession No. FJ985253) that lacks exons 5 and 7 and the first nucleotide of exon 6. This variant transcript also contains an intronic 42 bp insertion between exons 10 and 11 that is expressed “in-frame” from the start to stop codons, and contains intact SAND and MYND domains, but lacks the NLS domain encoded by exon 7 (Fig. 7a).

Characterization of the *Hu-DF1-VAR* isoform revealed a number of similarities with the mouse *DF1-VAR1* isoform. *Hu-DF1-VAR* was expressed predominantly in the cytoplasm (Fig. 7b) and did not mediate transcriptional activation of the 26 bp *Deaf1* response element (Fig. 7c). This variant interacted with canonical Hu-DF1 and altered its distribution within the cell. When expressed alone, Hu-DF1 localized almost exclusively in the nucleus (Fig. 7b, d), but when co-expressed with Hu-DF1-VAR its nuclear and cytoplasmic expression decreased by ~3-fold and increased by ~4-fold, respectively. On the other hand, co-expression of the two isoforms enhanced the nuclear localization of Hu-DF1-VAR (Fig. 7e).

To examine if the alternatively spliced isoform of *DEAF1* is upregulated in the PLN during T1D, QPCR was performed using primers that span the two deletion sites of the *Hu-DF1-VAR* transcript (Table 1 and Supplementary Fig. 7). Expression of *Hu-DF1-VAR* was ~20

fold higher in the PLN of T1D patients than in healthy controls (Fig. 7f). This finding strongly correlated with the lack of *INS* expression observed in the PLN of all T1D patients studied (Table 1). *INS* expression was detected in 4 of 5 of the control PLN, and in the spleen of all samples. The spleen samples expressed either no *Hu-DF1-VAR* or *Hu-DF1-VAR* amounts comparable to those detected in the control PLN (data not shown). Together, these data suggest that during the progression of human T1D, *DEAF1* is alternatively spliced to produce a nonfunctional variant similar to mouse DF1-VAR1. The Hu-DF1-VAR isoform interacts with and inhibits the transcriptional activity of canonical Hu-DF1 by retaining it in the cytoplasm.

Discussion

T1D develops from a breakdown in central or peripheral tolerance that is partially controlled by PTA expression in the thymus and lymph nodes, respectively. Here we demonstrate that Deaf1 plays a role in regulating PTA gene expression in peripheral lymphoid tissues. We found that the transcriptional activity of Deaf1 can be inhibited by alternatively spliced variants of Deaf1, and that the expression of these splice variants was significantly higher in the PLN of T1D patients and 12 week old NOD mice than in controls. These findings suggest that alternative splicing of *Deaf1* could play a key role in the pathogenesis of T1D and NOD disease.

The age of 12 weeks is pivotal in the progression of NOD disease, as infiltrative insulinitis and β -cell destruction begins at this age⁷. Peripheral tolerance to certain PTAs is facilitated in the lymph nodes through the ectopic expression of PTA genes in stromal cells^{2–4}, and defects in peripheral tolerance may induce infiltrative insulinitis. The expression of genes encoding various pancreatic PTAs is diminished in the PLN of NOD mice at 12 weeks of age⁵. This coincides with a downregulation of *DF1* and upregulation of *DF1-VAR1* gene expression. Since DF1-VAR1 inhibits PTA gene expression and interferes with the transcriptional activity of DF1, a change in Deaf1 isoform expression may result in decreased PTA expression in 12 week old NOD PLN and reduced tolerance to these antigens.

Due to the obvious practical difficulties in obtaining human PLN tissues from pre-diabetic individuals as well as those at disease onset, we could not assess the expression of *Hu-DF1* and *Hu-DF1-VAR* throughout all stages in the natural history of T1D. In the one pre-diabetic PLN sample we obtained, *Hu-DF1-VAR* expression was higher than in the PLN of all the healthy control samples examined. Interestingly, the increased expression of *Hu-DF1-VAR* and absence of *INS* in the PLN appeared to be maintained well after the onset of T1D.

Increased expression of the Deaf1 variant can inhibit the transcriptional activity of canonical Deaf1 by forming hetero-dimeric complexes that retain the canonical isoform in the cytoplasm. Both DF1-VAR1 and Hu-DF1-VAR lack the NLS domain that is required for nuclear localization and activation of gene transcription⁸, and both induced minimal transcriptional activity of the 26-bp Deaf1 response element compared to that induced by DF1 and Hu-DF1. The canonical isoform of Deaf1 is structurally similar to Aire, which also contains a SAND domain and can induce PTA gene expression by interacting with modified

and unmodified histone H3 via its PHD-ZF domain^{9, 10}. We suggest that Deaf1, rather than Aire, plays a role in controlling PTA expression in the PLN. Deaf1 may regulate PTA expression in a manner analogous to Aire since both proteins contain similar functional domains: Deaf1 contains a C-terminal ZF-MYND domain that is structurally similar to the PHD-ZF, as well as a SAND domain that functions as a DNA binding domain for chromatin-dependent transcription and a site for protein-protein interaction^{11, 12}. However, the effect of Deaf1 function may be cell-dependent. For example, Deaf1 represses and enhances promoter activity of the 5-HT1A receptor in presynaptic and postsynaptic neurons, respectively¹³. In addition, some genes were upregulated while others were downregulated in *Deaf1*-KO mice, suggesting that Deaf1 may interact with cell-specific regulatory factors to either stimulate or suppress gene transcription. The requirement for additional factors may explain why overexpression of DF1 did not significantly increase PTA gene expression in NIH 3T3 cells, and why changes in PTA gene expression in PLN tissue did not necessarily correlate with increased DF1 expression.

BALB/c mice, in which *Deaf1* was knocked out, did not manifest an obvious autoimmune phenotype. However, like Aire-KO mice, the serum of *Deaf1*-KO mice contained auto-antibodies that were immunoreactive against proteins in the retina of the eye¹. Interestingly, our microarray data showed that the most downregulated gene in the PLN of *Deaf1*-KO mice is *dopachrome tautomerase (Dct)*, which encodes a protein that is expressed exclusively in the retina. In addition, three other genes among the top 30 genes that were downregulated in the PLN of Deaf1 mice (*1500016O10Rik*, *Si*, and *Sgne1*) are expressed in the retina. The control of retinal antigen expression by Deaf1 may be of particular significance, as reduced antigen presentation in eye-draining lymph nodes prevents autoreactive T cell deletion and contributes to the development of retinal autoimmunity¹⁴.

Variations in thymic PTA gene expression can influence susceptibility to autoimmune disease^{15, 16}. The expression of genes encoding certain PTAs was reduced in the PLN of *Deaf1*-KO mice, while surprisingly, the expression the same genes and of *Aire* was increased in the thymus of the *Deaf1*-KO mice. This suggests the possibility that enhanced central tolerance mechanisms, mediated by increased Aire-regulated expression of PTAs in the thymus, may result in the lack of overt autoimmunity in the *Deaf1*-KO mice. Strain-dependent variations in the thymic expression of genes encoding certain PTAs, such as the uveitogenic retinal antigen interphotoreceptor retinoid binding promoter (IRBP), have been observed¹⁷. Previous studies have also shown that the severity of the autoimmune phenotype of Aire-knockout mice depends on the genetic background. Aire-deficient mice developed severe exocrine pancreatitis in NOD but not in C57BL/6 or BALB/c backgrounds¹⁸, while autoimmune gastritis and auto-antibodies against Mucin-6 developed in Aire-deficient mice in NOD and BALB/c backgrounds, but not in the C57BL/6 background¹⁹. The phenotype of the *Deaf1*-KO is also strain-specific. In the C57BL/6 background, *Deaf1*-KO mice suffered from various developmental defects that were not observed in BALB/c *Deaf1*-KO mice²⁰.

Ambp, *Fgb*, *Ppy* and *Reg3g* were downregulated in the PLN of *Deaf1*-KO mice, and we selected these genes for further study based on their regulation by Aire in the thymus¹ and reduced expression in the PLN of 12 week old NOD mice. In mTECs and LNSCs, PTAs are

expressed in low amounts. For example, PTA expression in lymph nodes was assessed using the iFABP-tOVA transgenic mouse model, where OVA (ovalbumin) represents a self-antigen expressed under the control of the fatty acid binding protein (FABP) promoter². OVA mRNA expression was detected in lymph nodes by RT-PCR, but OVA protein was not detected by immunoblotting. Similarly, PTA expression is low in the thymus, as only a small subset of mTECs ectopically express Aire and PTAs^{1, 21, 22}.

In humans, *INS* was not detected in the PLN of T1D patients, but was expressed in the PLN of healthy individuals and spleens of both control and T1D samples. The lack of *INS* expression correlated well with the high expression of *Hu-DF1-VAR* expressed in the PLN of T1D patients. In 12-week old NOD PLN, *Ins2* gene expression was also reduced, but we could not detect a difference in *Ins2* mRNA expression in the PLN of *Deaf1*-KO mice compared to BALB/c control mice. This may be due to the significantly lower expression of *Ins2* mRNA in the PLN of *Deaf1*-KO and BALB/c control mice (30 to 1700-fold lower) compared to that of NOD and NOD.B10 mice.

Members of the Reg family have been described as autoantigens in T1D, and the inflammation-induced upregulation of *Reg* expression in islets was suggested to contribute to the premature onset of diabetes²³. We showed that *Reg3g* expression was downregulated in the PLN of *Deaf1*-KO mice and 12-week old NOD mice, but were unable to determine if *Deaf1* directly regulated *Reg3g* expression since the NIH 3T3 and LN CD45⁻ cell lines that we used for the siRNA experiments did not express measurable amounts of *Reg3g*. A loss of endogenous PTA gene expression has been shown to occur in cultured mTEC²⁴ and LNSC lines (unpublished data). Thus, future experiments involving monoclonal antibodies to DF1-VAR1 and/or in situ hybridization studies of primary lymph node stromal elements derived from the PLN of NOD and NOD.B10 mice may be necessary to identify the actual stromal cell that expresses the variant *Deaf1* isoforms and to determine the direct role of *Deaf1* in the expression of PTA genes.

While the expression of *Ambp*, *Fgb*, *Ppy*, and *Reg3g* is regulated by Aire in the thymus, the expression of these genes in the PLN is more likely regulated by *Deaf1*. *Aire* expression was not altered in the PLN of *Deaf1*-KO mice or NOD mice, and most of the PTAs regulated by Aire in eTACs appear to be distinct from those regulated by *Deaf1* in the PLN.

Our study suggests that *Deaf1* promotes the ectopic expression of genes encoding PTAs in the PLN, and PTA expression in LNSCs can mediate peripheral tolerance². Thus, fine-tuning of peripheral tolerance, at least in the PLN, may occur through alternative splicing of *Deaf1*. Alternative splicing is a mechanism that is often used to control immune responses. However, variations in splicing can impair immune function and contribute to various autoimmune diseases²⁵. It is unclear how splicing of *Deaf1* is controlled, but inflammation of the NOD PLN may be involved since various inflammatory cytokines have been shown to induce alternative splicing^{26–30}. Differences in *Deaf1* splicing in NOD vs. NOD.B10 mice may also be due to other genes within the *Idd1* susceptibility region, a MHC congenic interval that distinguishes the two strains. Allelic variation of such genes or differences in their regulatory regions may influence their expression or function, which may be associated with splicing events.

We propose that during the progression of T1D and NOD disease, alternative splicing of *Deaf1* occurs in the PLN. The alternatively spliced *Deaf1* variant interacts with and retains the canonical isoform in the cytoplasm and inhibits PTA gene expression. Decreased expression of pancreatic antigens in the PLN may impair peripheral tolerance and lead to the survival of autoreactive T cells specific for these antigens. Thus, we suggest that differences in the expression of *Deaf1* isoforms in the PLN of humans with T1D and NOD mice may contribute to the development of this disease.

Supplementary Material

Refer to Web version on PubMed Central for supplementary material.

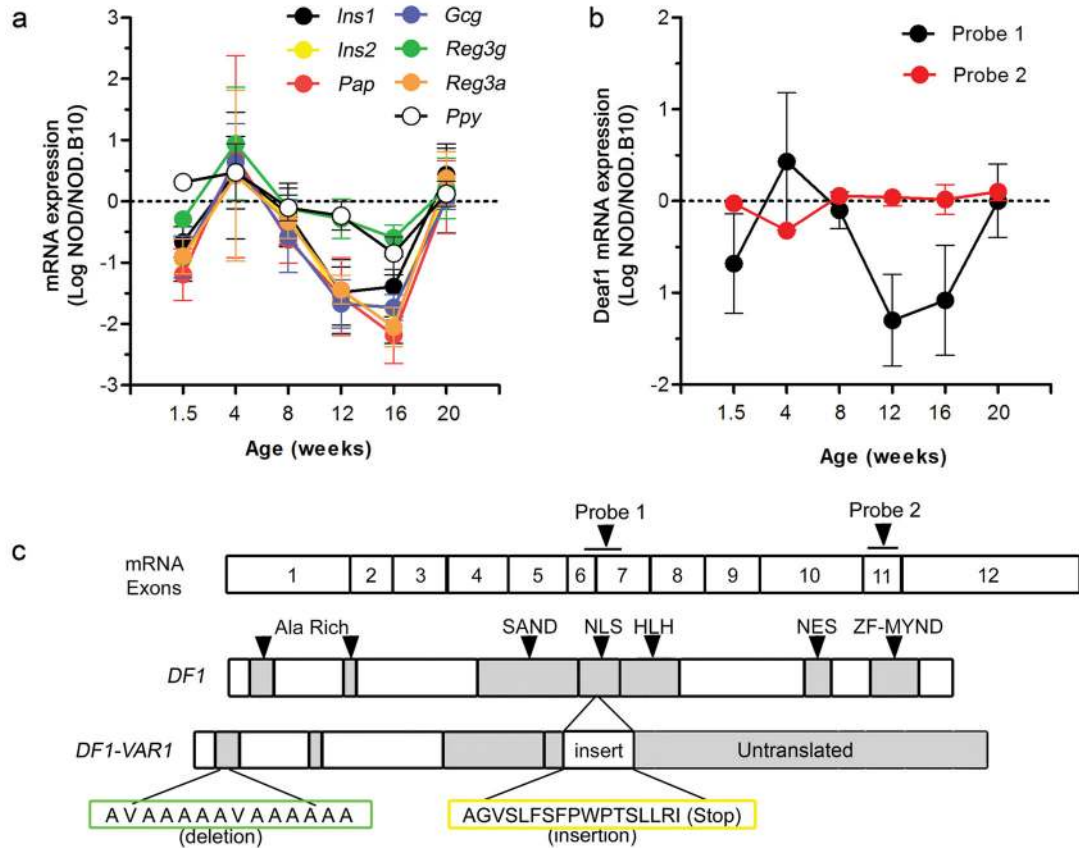
Acknowledgments

The authors would like to thank H. Iwai and C. Taylor for their technical assistance, J. Visvader (The Walter and Eliza Hall Institute of Medical Research) for providing *Deaf1*-KO mice, and the JDRF nPOD for providing human PLN and spleen samples. This work was funded by NIH grants UO1 DK078123-03, U19-DK 61934 and U19-AI050864 (to C.G.F.), and the Canadian Institutes of Health Research (CIHR; to P.R.A). Linda Yip was supported by the American Diabetes Association Mentor-based Postdoctoral Fellowship; Margaret Czesak received a CIHR Studentship.

References

1. Anderson MS, et al. Projection of an immunological self shadow within the thymus by the aire protein. *Science*. 2002; 298:1395–1401. [PubMed: 12376594]
2. Lee JW, et al. Peripheral antigen display by lymph node stroma promotes T cell tolerance to intestinal self. *Nat Immunol*. 2007; 8:181–190. [PubMed: 17195844]
3. Gardner JM, et al. Deletional tolerance mediated by extrathymic Aire-expressing cells. *Science*. 2008; 321:843–847. [PubMed: 18687966]
4. Nichols LA, et al. Deletional self-tolerance to a melanocyte/melanoma antigen derived from tyrosinase is mediated by a radio-resistant cell in peripheral and mesenteric lymph nodes. *J Immunol*. 2007; 179:993–1003. [PubMed: 17617591]
5. Kodama K, et al. Tissue- and age-specific changes in gene expression during disease induction and progression in NOD mice. *Clin Immunol*. 2008; 129:195–201. [PubMed: 18801706]
6. Lemonde S, et al. Impaired repression at a 5-hydroxytryptamine 1A receptor gene polymorphism associated with major depression and suicide. *J Neurosci*. 2003; 23:8788–8799. [PubMed: 14507979]
7. Adorini L, Gregori S, Harrison LC. Understanding autoimmune diabetes: insights from mouse models. *Trends Mol Med*. 2002; 8:31–38. [PubMed: 11796264]
8. Huggenvik JI, et al. Characterization of a nuclear deformed epidermal autoregulatory factor-1 (DEAF-1)-related (NUDR) transcriptional regulator protein. *Mol Endocrinol*. 1998; 12:1619–1639. [PubMed: 9773984]
9. Koh AS, et al. Aire employs a histone-binding module to mediate immunological tolerance, linking chromatin regulation with organ-specific autoimmunity. *Proc Natl Acad Sci U S A*. 2008; 105:15878–15883. [PubMed: 18840680]
10. Org T, et al. The autoimmune regulator PHD finger binds to non-methylated histone H3K4 to activate gene expression. *EMBO Rep*. 2008; 9:370–376. [PubMed: 18292755]
11. Jensik PJ, Huggenvik JI, Collard MW. Identification of a nuclear export signal and protein interaction domains in deformed epidermal autoregulatory factor-1 (DEAF-1). *J Biol Chem*. 2004; 279:32692–32699. [PubMed: 15161925]
12. Bottomley MJ, et al. The SAND domain structure defines a novel DNA-binding fold in transcriptional regulation. *Nat Struct Biol*. 2001; 8:626–633. [PubMed: 11427895]

13. Czesak M, Lemonde S, Peterson EA, Rogaeva A, Albert PR. Cell-specific repressor or enhancer activities of Deaf-1 at a serotonin 1A receptor gene polymorphism. *J Neurosci*. 2006; 26:1864–1871. [PubMed: 16467535]
14. Lambe T, et al. Limited peripheral T cell anergy predisposes to retinal autoimmunity. *J Immunol*. 2007; 178:4276–4283. [PubMed: 17371984]
15. Bennett ST, et al. Susceptibility to human type 1 diabetes at IDDM2 is determined by tandem repeat variation at the insulin gene minisatellite locus. *Nat Genet*. 1995; 9:284–292. [PubMed: 7773291]
16. Egwuagu CE, Charukamnoetkanok P, Gery I. Thymic expression of autoantigens correlates with resistance to autoimmune disease. *J Immunol*. 1997; 159:3109–3112. [PubMed: 9317106]
17. Avichezer D, et al. An immunologically privileged retinal antigen elicits tolerance: major role for central selection mechanisms. *J Exp Med*. 2003; 198:1665–1676. [PubMed: 14657219]
18. Venanzi ES, Melamed R, Mathis D, Benoist C. The variable immunological self: genetic variation and nongenetic noise in Aire-regulated transcription. *Proc Natl Acad Sci U S A*. 2008; 105:15860–15865. [PubMed: 18838677]
19. Gavanescu I, Kessler B, Ploegh H, Benoist C, Mathis D. Loss of Aire-dependent thymic expression of a peripheral tissue antigen renders it a target of autoimmunity. *Proc Natl Acad Sci U S A*. 2007; 104:4583–4587. [PubMed: 17360567]
20. Hahn K, et al. Defective neural tube closure and anteroposterior patterning in mice lacking the LIM protein LMO4 or its interacting partner Deaf-1. *Mol Cell Biol*. 2004; 24:2074–2082. [PubMed: 14966286]
21. Derbinski J, et al. Promiscuous gene expression in thymic epithelial cells is regulated at multiple levels. *J Exp Med*. 2005; 202:33–45. [PubMed: 15983066]
22. Derbinski J, Schulte A, Kyewski B, Klein L. Promiscuous gene expression in medullary thymic epithelial cells mirrors the peripheral self. *Nat Immunol*. 2001; 2:1032–1039. [PubMed: 11600886]
23. Planas R, et al. Reg (regenerating) gene overexpression in islets from non-obese diabetic mice with accelerated diabetes: role of IFNbeta. *Diabetologia*. 2006; 49:2379–2387. [PubMed: 16900387]
24. Kasai M, Kropshofer H, Vogt AB, Kominami E, Mizuochi T. CLIP-derived self peptides bound to MHC class II molecules of medullary thymic epithelial cells differ from those of cortical thymic epithelial cells in their diversity, length, and C-terminal processing. *Eur J Immunol*. 2000; 30:3542–3551. [PubMed: 11169395]
25. Lynch KW. Consequences of regulated pre-mRNA splicing in the immune system. *Nat Rev Immunol*. 2004; 4:931–940. [PubMed: 15573128]
26. Eissa NT, et al. Alternative splicing of human inducible nitric-oxide synthase mRNA. tissue-specific regulation and induction by cytokines. *J Biol Chem*. 1996; 271:27184–27187. [PubMed: 8900212]
27. Gratchev A, et al. Alternatively activated macrophages differentially express fibronectin and its splice variants and the extracellular matrix protein betaIG-H3. *Scand J Immunol*. 2001; 53:386–392. [PubMed: 11285119]
28. Borsi L, Castellani P, Risso AM, Leprini A, Zardi L. Transforming growth factor-beta regulates the splicing pattern of fibronectin messenger RNA precursor. *FEBS Lett*. 1990; 261:175–178. [PubMed: 2307231]
29. Togo S, Shimokawa T, Fukuchi Y, Ra C. Alternative splicing of myeloid IgA Fc receptor (Fc alpha R, CD89) transcripts in inflammatory responses. *FEBS Lett*. 2003; 535:205–209. [PubMed: 12560105]
30. Cowling RT, et al. Effects of cytokine treatment on angiotensin II type 1A receptor transcription and splicing in rat cardiac fibroblasts. *Am J Physiol Heart Circ Physiol*. 2005; 289:H1176–1183. [PubMed: 15879490]
31. Creusot RJ, et al. Tissue-targeted therapy of autoimmune diabetes using dendritic cells transduced to express IL-4 in NOD mice. *Clin Immunol*. 2008; 127:176–187. [PubMed: 18337172]

**Fig. 1.**

PTA and *Deaf1* isoform expression in the PLN of NOD mice. **a**) Expression of pancreatic PTAs in the PLN of NOD versus NOD.B10 mice, as assessed by microarray analysis. **b**) *Deaf1* mRNA expression in the PLN of NOD mice, as detected by Probe 1 and Probe 2 using microarray analysis. Data in panels **a** and **b** represent the mean log ratio of (NOD/NOD.B10) \pm s.d. ($n = 10$). **c**) Two isoforms of *Deaf1* (*DF1* and *DF1-VAR1*) were cloned from the PLN of 12 week old NOD mice. *DF1* hybridizes to Probe 1 and 2, while *DF1-VAR1* only hybridizes to Probe 2. *DF1-VAR1* contains a deletion in the N-terminal alanine-rich region and a partial intronic insertion between exon 6 and 7 that introduces a premature stop codon. Abbreviations: Ala (alanine); SAND (Sp100,AIRE-1-NucP41/75,DEAF-1); NLS (nuclear localization signal); NES (nuclear export signal); Zf-MYND (zinc finger-Myeloid, Nervy, and DEAF-1).

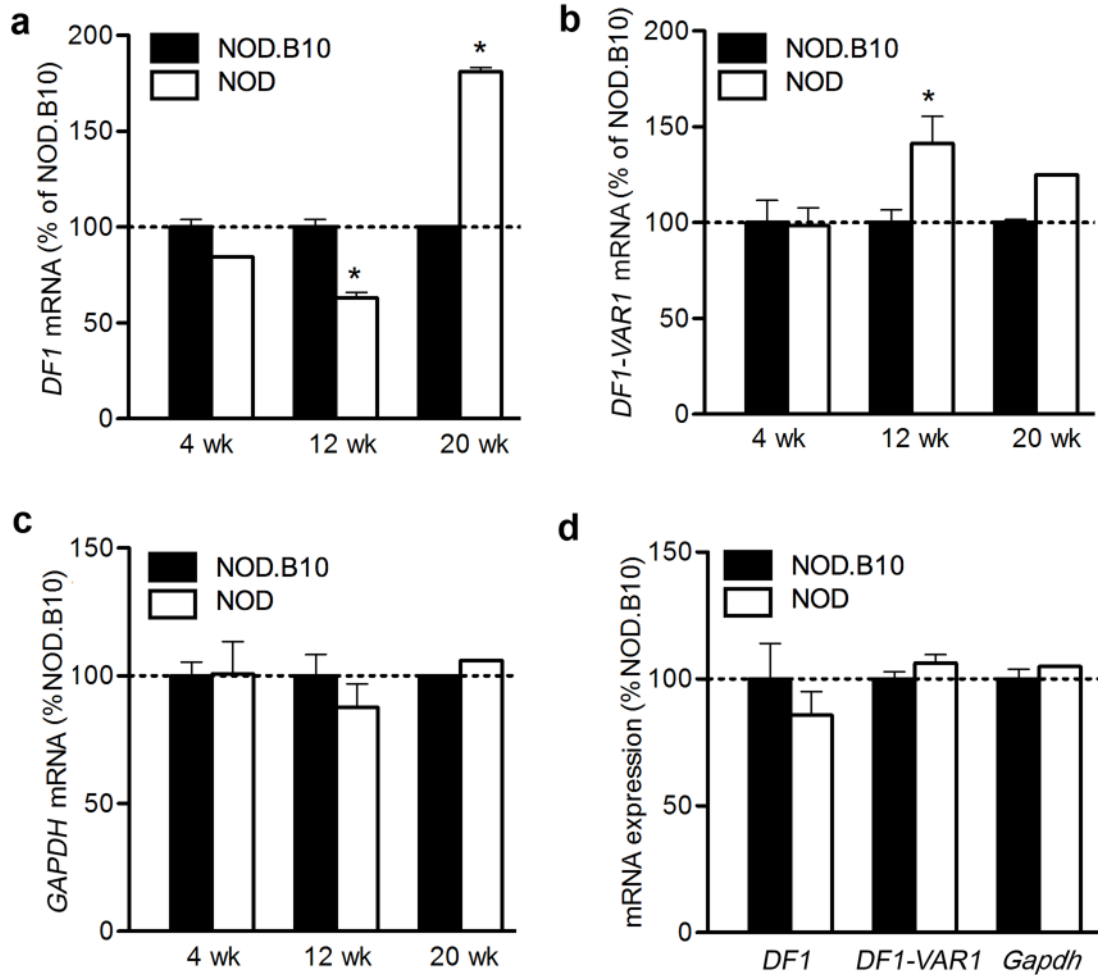


Fig. 2.

Quantification of *DF1* and *DF1-VAR1* gene expression in NOD PLN. *DF1* (a), *DF1-VAR1* (b) and *Gapdh* (c) gene expression was measured in 4, 12, and 20 week NOD and NOD.B10 PLN samples. (d) *DF1*, *DF1-VAR1* and *Gapdh* mRNA was measured in 12 week NOD and NOD.B10 spleen samples. Gene expression was normalized to *Actb* mRNA. Values represent the mean \pm SEM. * $P < 0.05$. P -values were determined using the Student's unpaired t-test, two-tailed. $n \geq 5$ for all groups.

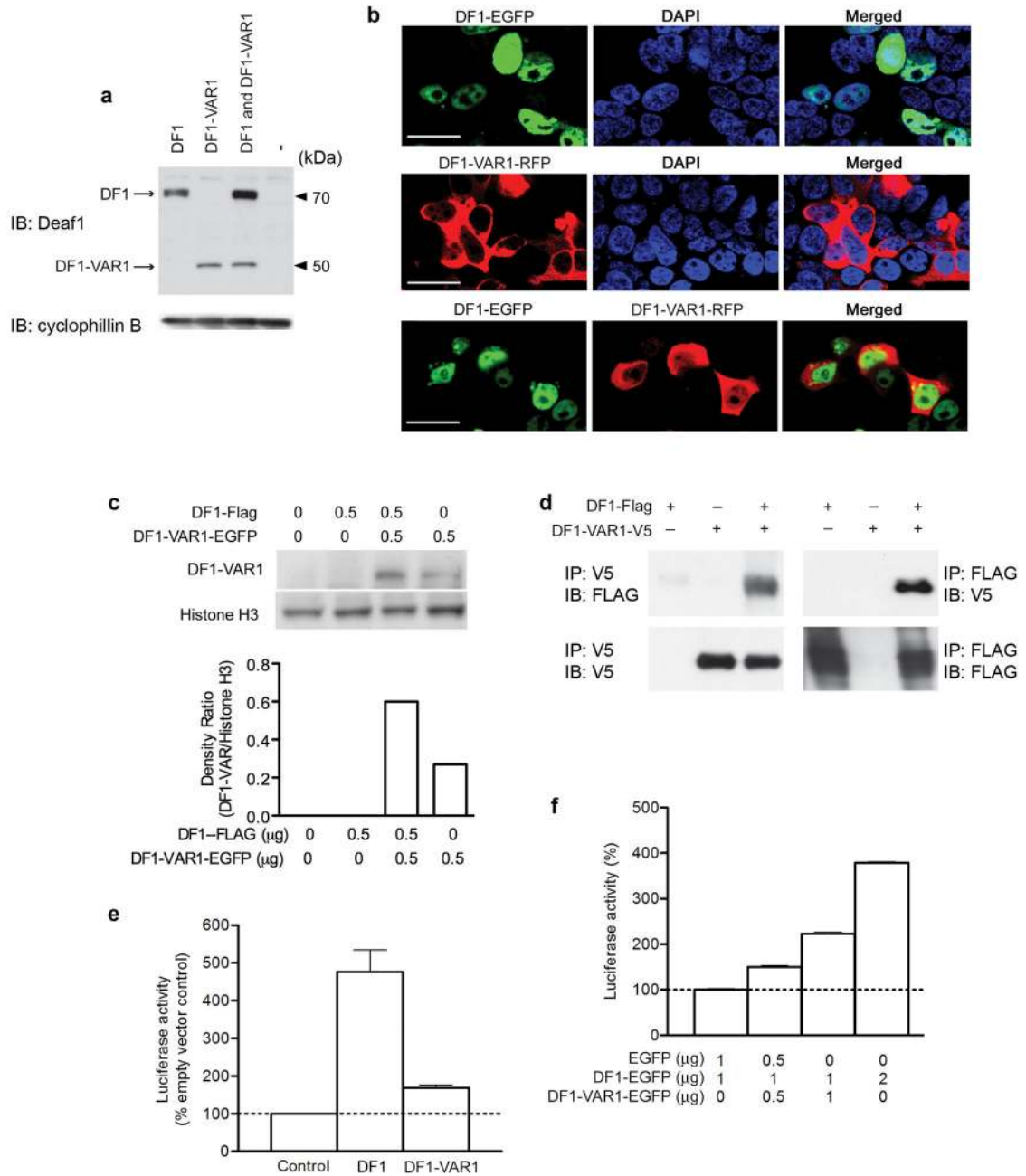


Fig. 3. Cellular localization, hetero-dimerization and transcriptional activity of DF1 and DF1-VAR1. **a**) Immunoblot of HEK 293 whole cell lysates transfected with 1 μg of DF1-Flag, DF1-VAR1-EGFP, 1 μg of both plasmids or empty control plasmid. Both DF1 (~70 kDa) and DF1-VAR1 (~50 kDa) were recognized by the Deaf1 antibody used. Cyclophilin B expression was assessed as a loading control. **b**) Confocal images showing the subcellular localization of EGFP-tagged DF1 and turbo-RFP-tagged DF1-VAR1 in DAPI-stained HEK 293 cells. Scale bar = 20 nm; images are representative of more than 100 similar cells. **c**) Immunoblot of nuclear lysates extracted from HEK 293 cells transfected with 0 or 0.5 μg of

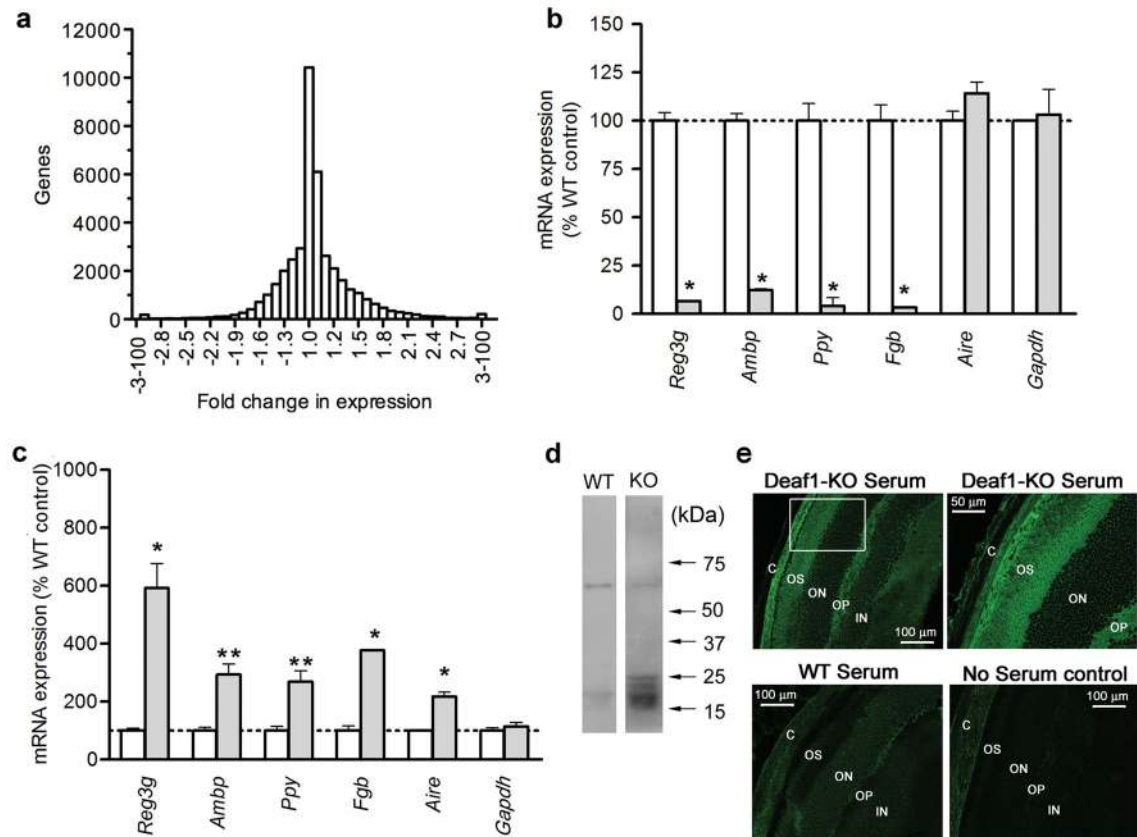
DF1-Flag and/or DF1-VAR1-EGFP. The nuclear marker histone H3 expression was assessed as a loading control. The densitometric ratio of DF1-VAR1 to histone H3 for each of these samples is shown below. Data is representative of 4 separate experiments. **d)** Co-immunoprecipitation assay. HEK 293 cells were transfected with the indicated Flag- or V5-tagged DF1 constructs. Lysates were subjected to immunoprecipitation and immunoblot with the indicated antibodies. **e,f)** Transcriptional activity of DF1 and DF1-VAR1 (or empty EGFP control vector) alone or in combination, as assessed using the 26 bp Deaf1-response element-luciferase reporter plasmid. Data in panel **c–f** are representative of similar results obtained in 3 separate experiments.

Author Manuscript

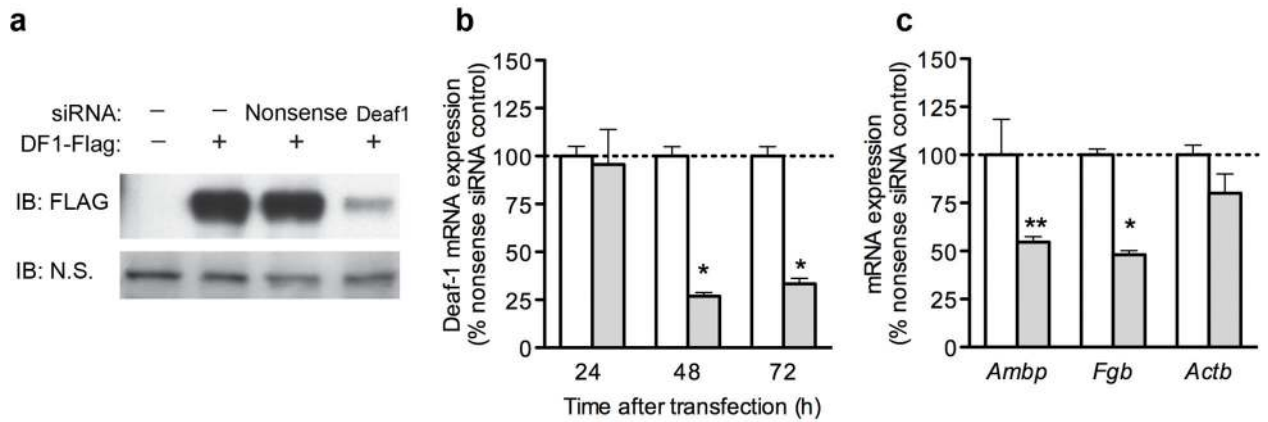
Author Manuscript

Author Manuscript

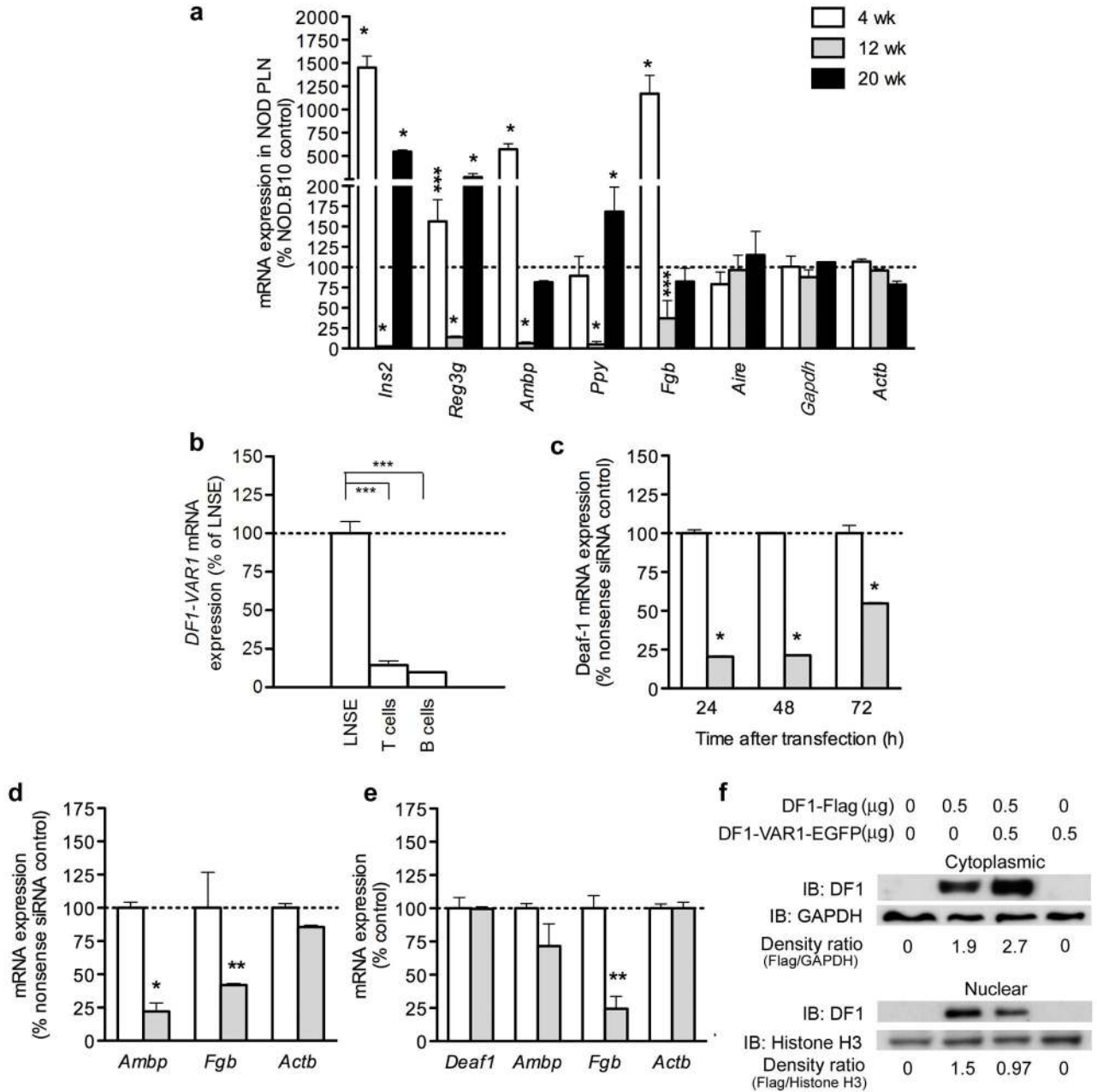
Author Manuscript

**Fig. 4.**

Analysis of *Deaf1*-KO mice. **(a)** Microarray analysis was used to identify genes that are upregulated and downregulated in the PLN of *Deaf1*-KO mice. Graph shows fold change in gene expression in PLN of BALB/c *Deaf1*-KO compared to BALB/c wild-type mice. ($n = 2$) **(b,c)** Quantitative PCR (QPCR) was used to measure gene expression differences in BALB/c *Deaf1*-KO (filled bars) versus BALB/c wild-type PLN (white bars; **b**) and thymus (**c**). Gene expression was measured in triplicate by QPCR and normalized with *18S rRNA* expression. Values represent the mean \pm SEM, $n = 4$ in each group. * $P \leq 0.001$; ** $P \leq 0.01$, Student's unpaired t-test, two-tailed. **(d)** Serum of 30 wk old *Deaf1*-KO or wild-type BALB/c mice was used for immunoblotting of mouse eye lysates. Data are representative of 3 similar experiments. **(e)** Confocal images of indirect immunofluorescence experiments performed in the mouse eye. Tissue sections (5 μ m) were incubated with diluted serum (1:100) from *Deaf1*-KO or wild-type littermate controls or with no serum (negative control), followed by Alexa-488 conjugated anti-mouse IgG (1:2000). A high magnification image of the boxed region is shown in the top right panel. (Abbreviations: OS = outer segment; OP = outer plexiform; C = choroid; ON = outer nuclear layer; IN = inner nuclear layer). Data is representative of 12 sections per group.

**Fig. 5.**

Deaf1 regulates gene expression in NIH 3T3 cells. NIH 3T3 cells were co-transfected with Deaf1 or nonsense siRNA and with *DF1-Flag*. **(a)** The expression of exogenous Deaf1 was assessed by immunoblot with anti-Flag. A non-specific band (N.S.) was used as a loading control. **(b, c)** Expression of the indicated endogenous mRNA transcripts was measured by QPCR at indicated times after transfection **(b)** or at 48 h after transfection **(c)**. Cells transfected with nonsense siRNA and *Deaf1* siRNA are indicated by white and grey bars, respectively. Gene expression was measured in triplicate by QPCR and normalized with *18S rRNA* expression. Values represent the mean \pm SEM of 3 separate experiments. * $P \leq 0.001$; ** $P \leq 0.05$, Student's unpaired t-test, two-tailed.

**Fig. 6.**

Regulation of PTA expression in NOD PLN and LN CD45⁻ cells by Deaf1 and DF1-VAR1.

a) Gene expression of PTAs in the PLN of NOD versus NOD.B10 mice at various ages ($n \geq 4$ per group). Data are normalized with *18S rRNA* expression and presented as a percent of age-matched NOD.B10 controls. **b**) Relative expression of *DF1-VAR1* mRNA in various cells isolated from the 12-week NOD PLN ($n = 3$). Expression was normalized to *Actb*. **c**) *DF1* mRNA expression in LN CD45⁻ cells transfected with Deaf1 or nonsense siRNA ($n = 3$) was measured by QPCR at the indicated times after transfection. **d**) LN CD45⁻ cells were transfected with Deaf1 or nonsense siRNA and expression of the indicated mRNA

transcripts was measured by QPCR 48 h after transfection ($n \geq 4$). For **c** and **d**, cells transfected with nonsense siRNA and *Deaf1* siRNA are indicated by white and grey bars, respectively. **e**) LN CD45⁻ cells were infected with viral particles carrying *DF1-VARI* (grey bars) or an empty control plasmid (white bars), and mRNA expression was measured 72 h later ($n = 3$). Gene expression was measured in triplicate and normalized with *18S rRNA* expression. Values represent the mean \pm SEM. *** $P \leq 0.001$; ** $P \leq 0.01$; * $P \leq 0.05$, Student's unpaired t-test, two-tailed. **f**) HEK 293 cells were transfected with *DF1-Flag* and/or *DF1-VARI-EGFP*. Cytoplasmic and nuclear extracts were prepared and analyzed by immunoblot. The cytoplasmic marker Gapdh and nuclear marker histone H3 were used as loading controls. Data are representative of 4 similar experiments.

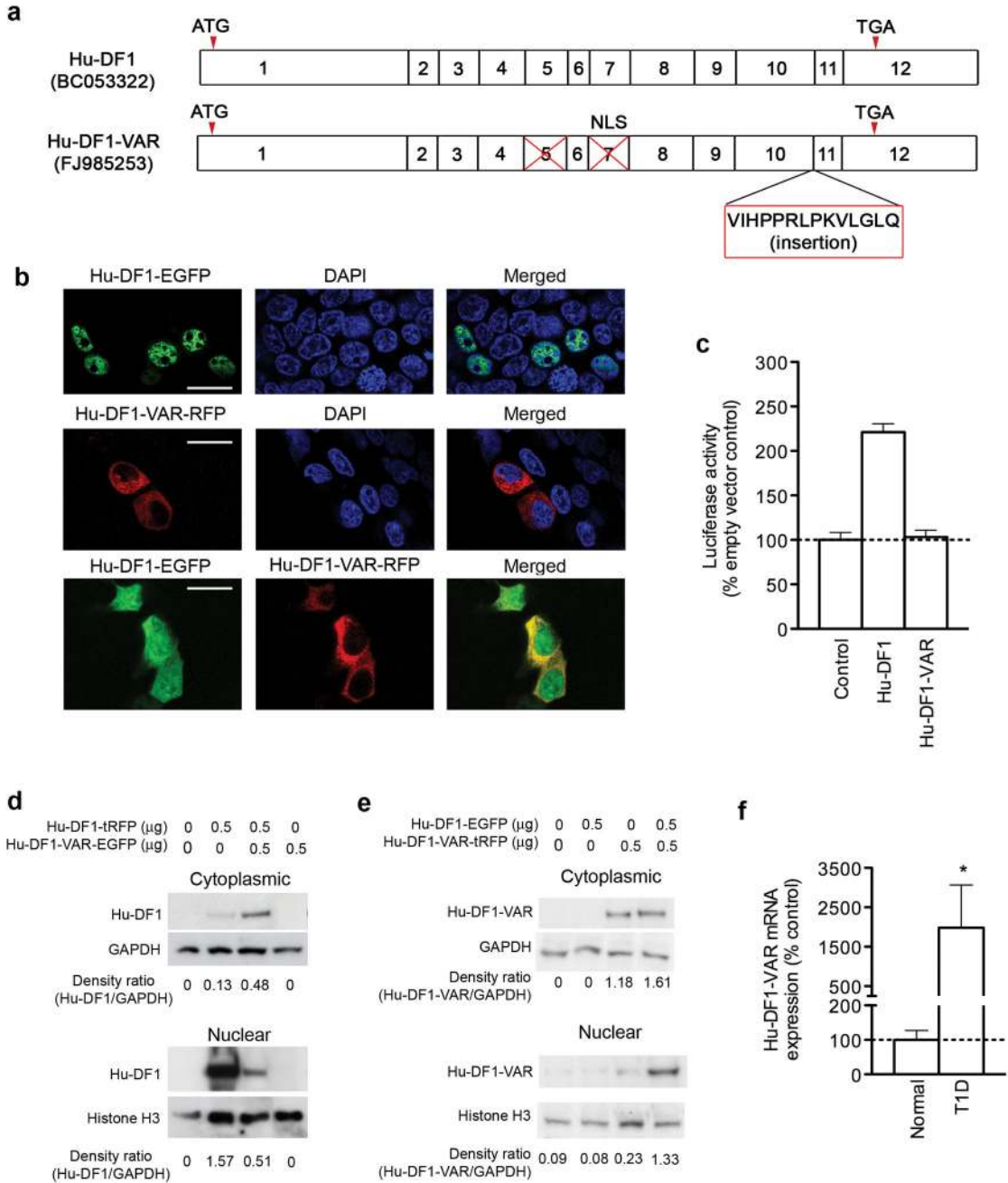


Fig. 7. Identification and characterization of an alternatively spliced *DEAF1* isoform in human PLN. **a**) Two *DEAF1* isoforms were cloned from human PLN, a canonical *DEAF1* transcript (*Hu-DF1*) and an alternatively spliced variant (*Hu-DF1-VAR*). **b**) Confocal images showing the subcellular localization of EGFP-tagged *Hu-DF1* and turbo-RFP-tagged *Hu-DF1-VAR* in DAPI-stained HEK 293 cells. Scale bar = 30 nm; images are representative of more than 100 similar cells. **c**) The transcriptional activity of *Hu-DF1* and *Hu-DF1-VAR* was assessed in HEK 293 cells using the 26 bp *Deaf1*-response element-luciferase reporter plasmid. Data

are representative of 2 similar experiments. **(d,e)** HEK 293 cells were transfected with *Hu-DF1-turboRFP* and/or *Hu-DF1-VAR-EGFP*. Cytoplasmic and nuclear extracts were prepared and analyzed by immunoblot. The cytoplasmic marker GAPDH and nuclear marker histone H3 were used as loading controls. Data are representative of 3 similar experiments. **f)** Quantification of *Hu-DF1-VAR* gene expression in the PLN of healthy and T1D patients by QPCR. ($n = 5$; $*P < 0.02$, Mann Whitney test, two-tailed).

Author Manuscript

Author Manuscript

Author Manuscript

Author Manuscript

Table 1

INS gene expression in the PLN and SPL of T1D and control patients

Group	Age	Sex	PLN*	SPL
Control	24	F	+	n/a
Control	30	M	+	n/a
Control	32	F	-	n/a
Control	30	M	+	+
Control	41	M	+	+
T1D	32	M	-	+
T1D	76	M	-	+
T1D	37	F	-	+
T1D	28	F	-	+
Pre-T1D	7	M	-	+

* QPCR threshold cycles of > 37 were considered negative. Measurements were performed in triplicate and data are representative of ≥ 2 separate experiments.